Square deployable frames for space applications. Part 1: theory

Y Chen[1] and **Z You**[2*]
[1]School of Mechanical and Aerospace Engineering, Nanyang Technological University, Singapore
[2]Department of Engineering Science, University of Oxford, Oxford, UK

The manuscript was received on 2 December 2005 and was accepted after revision for publication on 3 March 2006.

DOI: 10.1243/09544100JAERO68

Abstract: The Bennett linkage is a three-dimensional 4R overconstrained mechanism consisting of four rigid links connected by revolute hinges whose axes of rotation are neither parallel nor concurrent. In general, it cannot be folded up compactly. This paper investigates the existence of alternative forms of the linkage in order to achieve the most compact folding and maximum expansion so that the linkage can be used as basic building blocks of large deployable structures for aerospace applications. This study has resulted in the creation of an effective deployable element based on the Bennett linkage. A simple method to build the Bennett linkage in its alternative form has been introduced and verified. The corresponding networks have been obtained following a layout similar to that the original Bennett linkage, which the authors discovered previously. This approach can also be extended to other types of overconstrained linkages so that they can be used for building large deployable assemblies as well.

Keywords: deployable structure, Bennett linkage, bar assembly, alternative form

1 INTRODUCTION

Many aerospace structures expand to a flat profile. Typical examples include solar blankets and arrays as well as some of the reflector antennas [**1**]. Such a structure could either be supported by a set of expandable beams radially spanning from a central hub or by a frame structure along its edges. The supporting structures can be made from self-rigidizing inflatable tubes, flexible tubes unrolled from a folded package, or foldable frame structures. The latter are often linkages. By activating the mobilities existing in a linkage, the structure can expand from a compact bundle. This paper deals with this type of structures.

The use of linkages for space applications is not new. Deployable structures built from basic mechanisms are commonly used as the backbone for masts, solar panels, and antennas. They may have one or more degrees of freedom. To avoid complex control system, it is often desirable in some circumstances to have structures with only a single internal mobility so that the deployment operations can be greatly simplified. The combination of single degree of mobility and requirement of high structural stiffness without many latching devices means that it is ideal to adopt overconstrained linkages. Early examples of such structures include the variable geometry (VG) trusses [**2**], the tetrahedral truss [**3**], the Panctruss [**4**], and the mesh reflector [**5**].

Utilization of overconstrained mechanisms for the design of deployable structures involves the identification of suitable mechanisms and the development of a suitable layout by which each individual mechanism can be connected while retaining the mobility. This process can be illustrated by the x-beam concept [**6**]. It is a mast consisting of a series of Sarrus linkages. The structural arrangement allows the mobility of each Sarrus linkage to be retained, and the retraction of the beam is accomplished by a system of cables passing through pulleys mounted onto the structure.

Most of the structures developed through this route use only two-dimensional mechanisms as basic building blocks, which are placed on different planes to create three-dimensional structures. Mathematically, it is much easier to ensure geometrical

Corresponding author: Department of Engineering Science, University of Oxford, Parks Road, Oxford, Oxfordshire OX1 3PJ, UK. email: zhong.you@eng.ox.ac.uk

compatibility. Deployable structures utilizing three-dimensional mechanisms are rare in spite of large number of three-dimensional overconstrained linkages invented by Bennett [**7**], Goldberg [**8**], Waldron [**9**], Wohlhart [**10**], Mavroidis and Roth [**11**], Diermeier [**12**] and so on. A noticeable exception is the x-beam mentioned earlier by Adams [**6**]. Most three-dimensional overconstrained linkages exhibiting fascinating mathematical features have been found to be of little use in practice.

Since 2000, the authors have been attempting to construct a mobile grid using three-dimensional overconstrained linkages. The authors have discovered that it is possible to build deployable grids with a single mobility using the Bennett and Bricard [**13**, **14**]. However, structures based on the Bennett linkage are unable to be retracted compactly, rendering them less useful for aerospace applications in which compact folding is one of the most important requirements.

The objective of the current study is to explore the possibility of achieving the most effective folding and deployment for the deployable structures based on the Bennett linkage. The strategy is to construct the Bennett linkages using the alternative forms. The mathematical representation of the Bennett linkage defines the length of the rigid links as the shortest distance between two adjacent axes. The links are always perpendicular to the axes at their ends, which is *the original form*. In *the alternative form*, the axes of the revolute joints are extended and the joints are connected with the links that are not perpendicular to the joint axes. It has been found that by doing so, the Bennett linkage can indeed be retracted to a bundle. Furthermore, the linkages in their alternative forms can be connected together just as those in their original forms.

The study is to be presented in two sister articles. The first article contains the geometrical theory showing the existence of the alternative forms of the Bennett linkage and their use as deployable frames, whereas the second deals with the construction issues of the frames.

The layout of the paper is as follows. It starts with a brief introduction of key geometrical properties of the Bennett linkage in section 2. The detailed derivation of the alternative form of the Bennett linkage is given in section 3, in which a solution giving the most compact folding as well as the maximum expansion is presented. An in-depth discussion in section 4 concludes the paper.

2 THE BENNETT LINKAGE

The Bennett linkage is a three-dimensional overconstrained linkage. It is remarkable because it is a loop consisting of only four pieces, the minimum number to form a useful mechanism, connected by revolute joints whose axes of rotation are neither parallel nor concurrent (Fig. 1). Bennett [**7**] identified the conditions for the linkage to have a single degree of mobility. If the length and the twist are defined as the shortest distance and the skew angle between the axes of two adjacent revolute joints, respectively, the conditions are as follows.

1. Two alternate links have the same length and the same twist, that is

$$a_{12} = a_{34} = a, \quad a_{23} = a_{41} = b$$
$$\alpha_{12} = \alpha_{34} = \alpha, \quad \alpha_{23} = \alpha_{41} = \beta$$

2. Lengths and twists should satisfy the condition

$$\frac{\sin\alpha}{a} = \frac{\sin\beta}{b}$$

The values of the revolute variables, θ_1, θ_2, θ_3, and θ_4, vary when the linkage moves, but

$$\theta_1 + \theta_3 = 2\pi, \quad \theta_2 + \theta_4 = 2\pi \tag{1}$$

and

$$\tan\frac{\theta_1}{2}\tan\frac{\theta_2}{2} = \frac{\sin 1/2(\alpha_{23} + \alpha_{12})}{\sin 1/2(\alpha_{23} - \alpha_{12})} \tag{2}$$

These three closure equations ensure that only one of the θ's is independent, so that the linkage has a single degree of mobility [**15**].

Taking $\theta_1 = \theta$ and $\theta_2 = \varphi$, equation (2) becomes

$$\tan\frac{\theta}{2}\tan\frac{\varphi}{2} = \frac{\sin 1/2(\beta + \alpha)}{\sin 1/2(\beta - \alpha)} \tag{3}$$

Bennett [**16**] also identified some special cases.

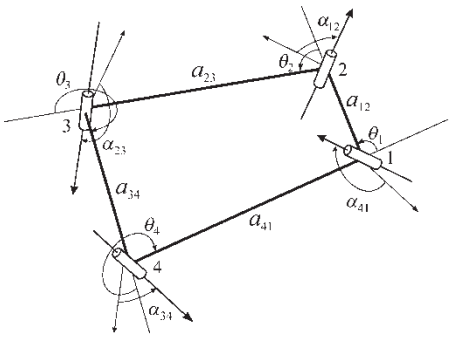

Fig. 1 A schematic diagram of the Bennett linkage

1. An equilateral linkage is obtained if $a = b$ and $\alpha + \beta = \pi$ (Fig. 2(a)). Equation (3) then becomes

$$\tan\frac{\theta}{2}\tan\frac{\varphi}{2} = \frac{1}{\cos\alpha} \tag{4}$$

2. If $\alpha = \beta$ and $a = b$, the four links are congruent. The motion is discontinuous: $\theta = \pi$ allows any value for φ and $\varphi = \pi$ allows any value for θ.

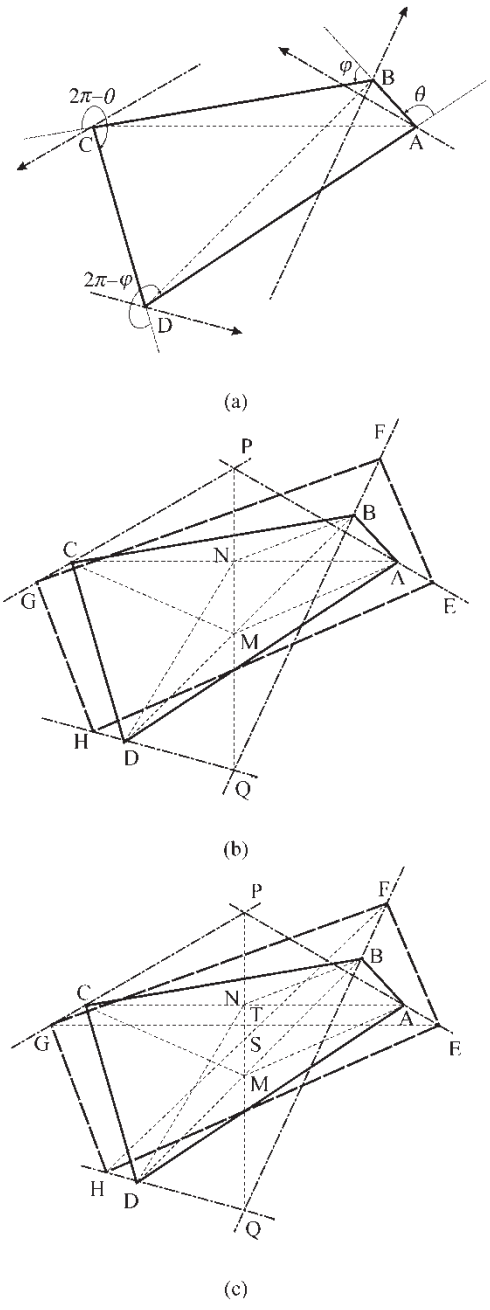

Fig. 2 Equilateral Bennett linkage. Certain new lines are introduced in (a), (b), and (c) for derivation of compact folding and maximum expansion conditions

3. If $\alpha = \beta = 0$, the linkage is a two-dimensional crossed isogram.
4. If $\alpha = 0$ and $\beta = \pi$, the linkage becomes a two-dimensional parallelogram.
5. If $a = b = 0$, the linkage is a spherical 4R linkage [**17**].

3 ALTERNATIVE FORMS OF THE BENNETT LINKAGE

For the equilateral Bennett linkage shown in Fig. 2(a), equation (4) indicates that φ must be close to π while θ approaches 0, or vice versa, which means that the distance between B and D becomes the smallest, whereas that between A and C is the largest. As a result, the Bennett linkage can be folded, but not simultaneously in both directions. However, the authors are to demonstrate that modification can be carried out to make compact folding possible.

Consider an equilateral special case of the Bennett linkage, where

$$a_{AB} = a_{BC} = a_{CD} = a_{DA} = l \tag{5}$$

$$\alpha_{AB} = \alpha_{CD} = \alpha, \quad \alpha_{BC} = \alpha_{DA} = \pi - \alpha \tag{6}$$

as shown in Fig. 2(a). For the purpose of geometric derivation, the joints of the Bennett linkage are marked with letters A, B, C, and D. The lengths and twists of linkage are also marked with letters in the subscripts. For instance, α_{AB} is the skew angle between joints A and B.

This linkage is symmetric about two planes: the first plane is normal to BD and through AC and the second plane passes through BD and normal to AC, even though lines AC and BD may not cross each other. The axes of revolute joints are marked as dash–dot lines at A, B, C, and D. The positive directions of the revolute axes are also shown in Fig. 2(a).

Denote the respective middle points of BD and AC by M and N (Fig. 2(b)). Obviously, ΔABD and ΔCDB are isosceles and identical triangles due to equation (5). Similarly are ΔBCA and ΔDAC. These lead to the conclusion that ΔAMC and ΔBND are both isosceles triangles. Hence, MN is perpendicular to both AC and BD. Furthermore, extensions of the axes of revolute joints must meet the extension of MN at P and Q, respectively, due to symmetry.

Consider four alternative connection points E, F, G, and H along the extensions of the revolute axes AP, BQ, CP, and DQ, respectively. To preserve symmetry, define

$$\overline{GC} = \overline{AE} = c \quad \text{and} \quad \overline{BF} = \overline{DH} = d \tag{7}$$

Hence

$$\overline{\mathrm{EF}}^2 = \overline{\mathrm{GH}}^2 = l^2 + c^2 + d^2 - 2cd\cos(\pi - \alpha_{\mathrm{AB}})$$
$$\overline{\mathrm{FG}}^2 = \overline{\mathrm{HE}}^2 = l^2 + c^2 + d^2 - 2cd\cos\alpha_{\mathrm{BC}} \tag{8}$$

Substituting equation (6) into equation (8) gives

$$\overline{\mathrm{EF}} = \overline{\mathrm{FG}} = \overline{\mathrm{GH}} = \overline{\mathrm{HE}} = \sqrt{l^2 + c^2 + d^2 + 2cd\cos\alpha} \tag{9}$$

which means EFGH is also equilateral.

For any given Bennett linkage ABCD, equation (9) shows that EF, FG, GH, and HE have constant length for given c and d. They do not vary with the revolute variables, θ and φ. Thus, it is possible to replace EF, FG, GH, and HE with bars connected by the revolute joints whose axes are along BF, CG, DH, and AE, respectively. EFGH is therefore an alternative form of the original Bennett linkage ABCD.

For each given set of c and d, an alternative form for the Bennett linkage can be obtained. The next step is to examine whether a particular form would provide the most compact folding.

When the linkage in the alternative form displaces, the distance between E and G varies. The distance between F and H also varies. Assume that when the structure is fully folded, deployment angles θ and φ become θ_{f} and φ_{f}, respectively. The condition for the most compact folding is

$$\overline{\mathrm{EG}} = \overline{\mathrm{FH}} = 0 \tag{10}$$

This means that physically the mechanism becomes a bundle.

Equation (10) can be written in terms of c, d, and the deployment angles. Consider ΔADC in Fig. 2(b). It can be found that

$$\overline{\mathrm{AC}}^2 = \overline{\mathrm{AD}}^2 + \overline{\mathrm{CD}}^2 - 2\overline{\mathrm{AD}}\cdot\overline{\mathrm{CD}}\cos(\pi - \varphi)$$
$$= 2l^2(1 + \cos\varphi) \tag{11}$$

Similarly, in ΔABD

$$\overline{\mathrm{BD}}^2 = \overline{\mathrm{AB}}^2 + \overline{\mathrm{AD}}^2 - 2\overline{\mathrm{AB}}\cdot\overline{\mathrm{AD}}\cos(\pi - \theta)$$
$$= 2l^2(1 + \cos\theta) \tag{12}$$

whereas in ΔBCM

$$\overline{\mathrm{CM}}^2 = \overline{\mathrm{BC}}^2 - \overline{\mathrm{BM}}^2 = \frac{l^2}{2}(1 - \cos\theta) \tag{13}$$

Thus, from ΔAMC

$$\cos\angle\mathrm{AMC} = 1 - 2\frac{1 + \cos\varphi}{1 - \cos\theta} \tag{14}$$

As segments DA and BA are perpendicular to AP, and so segment MA is also perpendicular to AP, from quadrilateral PAMC, it follows that

$$\cos\angle\mathrm{APC} = -\cos\angle\mathrm{AMC} = 2\frac{1 + \cos\varphi}{1 - \cos\theta} - 1 \tag{15}$$

Because in ΔAPC

$$\overline{\mathrm{AC}}^2 = 2\overline{\mathrm{PC}}^2(1 - \cos\angle\mathrm{APC})$$
$$= 4\overline{\mathrm{PC}}^2\frac{-\cos\theta - \cos\varphi}{1 - \cos\theta} \tag{16}$$

Comparing equations (11) and (16), the following equation is obtained

$$\overline{\mathrm{PC}}^2 = l^2\frac{(1 + \cos\varphi)(1 - \cos\theta)}{-2(\cos\varphi + \cos\theta)} \tag{17}$$

Similarly, it can be obtained that

$$\overline{\mathrm{QB}}^2 = l^2\frac{(1 + \cos\theta)(1 - \cos\varphi)}{-2(\cos\varphi + \cos\theta)} \tag{18}$$

In ΔEPG

$$\overline{\mathrm{EG}}^2 = 2(c + \overline{\mathrm{PC}})^2(1 - \cos\angle\mathrm{APC})$$
$$= 4(c + \overline{\mathrm{PC}})^2\frac{-\cos\theta - \cos\varphi}{1 - \cos\theta} \tag{19}$$

and similarly

$$\overline{\mathrm{FH}}^2 = 2(d + \overline{\mathrm{QB}})^2(1 - \cos\angle\mathrm{BQD})$$
$$= 4(d + \overline{\mathrm{QB}})^2\frac{-\cos\theta - \cos\varphi}{1 - \cos\varphi} \tag{20}$$

In general, ∠APC and ∠BQD cannot reach zero at the same time. Substituting equations (19) and (20) into equation (10) yields

$$c = -\overline{\mathrm{PC}} = -l\sqrt{\frac{(1 + \cos\varphi_{\mathrm{f}})(1 - \cos\theta_{\mathrm{f}})}{-2(\cos\varphi_{\mathrm{f}} + \cos\theta_{\mathrm{f}})}} \quad \text{and}$$
$$d = -\overline{\mathrm{QB}} = -l\sqrt{\frac{(1 - \cos\varphi_{\mathrm{f}})(1 + \cos\theta_{\mathrm{f}})}{-2(\cos\varphi_{\mathrm{f}} + \cos\theta_{\mathrm{f}})}} \tag{21}$$

The reason that both c and d are negative is due to the definition of these two parameters given in equation (7).

The above equations show how the values of c and d are related to the fully folded deployment angles θ_f and φ_f. In fact, c and d can be determined graphically as solutions (21) simply mean that E and G should move to a single point P, and F and H go to Q if the configuration shown Fig. 2(b) represents the fully folded configuration of the linkage EFGH.

Having obtained the linkage corresponding to the most efficient folding configuration, what is the form of the Bennett linkage that covers the largest area? To answer this question, it is necessary to find out the geometrical condition relating to the maximum coverage.

Figure 2(c) shows the alternative form of the Bennett linkage EFGH. Owing to symmetry, a line between E and G will intersect MN at T and that between F and H will intersect MN at S. The projection of EFGH will cover a maximum area if

$$\overline{ST} = 0 \tag{22}$$

when deployment angles reach θ_d and φ_d. This implies that EFGH is completely flattened to a rhombus.

Again, $\overline{ST}$ can be expressed in terms of c, d, and deployment angles. Based on equations (11) and (13)

$$\overline{MN}^2 = \overline{CM}^2 - \overline{CN}^2 = \overline{CM}^2 - \frac{\overline{AC}^2}{4} = -\frac{l^2}{2}(\cos\theta + \cos\varphi) \tag{23}$$

and equation (15) gives

$$\sin\angle PGE = \sin\left(\frac{\pi}{2} - \frac{1}{2}\angle APC\right) = \frac{\cos\varphi/2}{\sin\theta/2}$$

Therefore

$$\overline{NT} = c \cdot \sin\angle PGE = c \cdot \frac{\cos\varphi/2}{\sin\theta/2} \tag{24}$$

Similarly

$$\overline{MS} = d \cdot \sin\angle QFH = d \cdot \frac{\cos\theta/2}{\sin\varphi/2} \tag{25}$$

Hence, considering equations (23) to (25), $\overline{ST}$ can be written as

$$\overline{ST} = \overline{MN} - \overline{MS} - \overline{NT} = l\sqrt{-\frac{(\cos\theta + \cos\varphi)}{2}} - d\frac{\cos\theta/2}{\sin\varphi/2} - c\frac{\cos\varphi/2}{\sin\theta/2} \tag{26}$$

When $\theta = \theta_d$ and $\varphi = \varphi_d$

$$\overline{ST} = l\sqrt{-\frac{(\cos\theta_d + \cos\varphi_d)}{2}} - d\frac{\cos\theta_d/2}{\sin\varphi_d/2} - c\frac{\cos\varphi_d/2}{\sin\theta_d/2} = 0 \tag{27}$$

due to equation (22). Substituting c and d obtained from equation (21) into equation (27), using tangents of half-angles to express cosines, and considering equation (4), that is

$$\tan\frac{\theta_d}{2}\tan\frac{\varphi_d}{2} = \tan\frac{\theta_f}{2}\tan\frac{\varphi_f}{2} = \frac{1}{\cos\alpha} \tag{28}$$

results in

$$-\tan^2\alpha\tan\frac{\theta_d}{2}\tan\frac{\theta_f}{2} = \sec^2\frac{\theta_d}{2}\sec^2\frac{\theta_f}{2} + \tan^2\alpha \tag{29}$$

in which $0 \leqslant \theta_f \leqslant \pi$ and $\pi \leqslant \theta_d \leqslant 2\pi$.

Solutions to equation (29) only exist when the value of α is in the range between $\arccos(1/3)$ and $\pi - \arccos(1/3)$, i.e. 70.53°–109.47°. Within this range, the relationship between θ_d and θ_f for a set of given α is shown in Fig. 3. Note that in most circumstances, each θ_f corresponds to two values of θ_d. This means that there are two possible deployed configurations in which the structure built with the alternative forms of the Bennett linkage can be flattened. For $\alpha < \arccos(1/3)$ or $\alpha > \pi - \arccos(1/3)$, there is no pair of θ_f and θ_d satisfying equation (29). Therefore, the structure is incapable of being flattened, although it can still be folded up compactly.

From equation (9), the actual side length of the alternative form of the Bennett linkage, L, can be obtained as

$$L = \sqrt{l^2 + c^2 + d^2 + 2cd\cos\alpha} \tag{30}$$

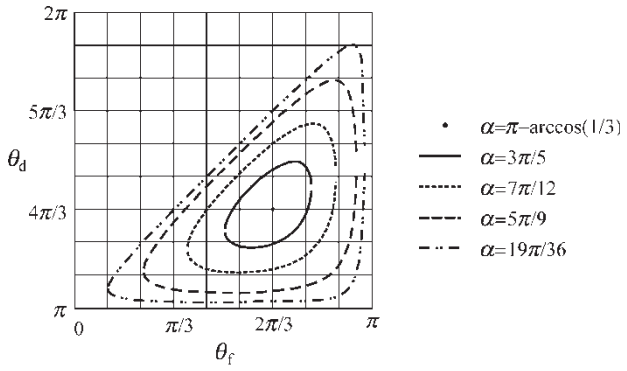

Fig. 3 θ_f versus θ_d for a set of given α

Substituting equation (21) into equation (30) results in

$$\frac{L}{l} = \sqrt{-\frac{2}{\cos\theta_{\mathrm{f}} + \cos\varphi_{\mathrm{d}}}} \tag{31}$$

Figure 4 shows the relationship between θ_{f} and L/l, c/l and d/l when $\alpha = 7\pi/12$.

Denote by δ the angle between two adjacent sides of the alternative form of the Bennett linkage in its flattened configuration when $\theta = \theta_{\mathrm{d}}$ and $\varphi = \varphi_{\mathrm{d}}$. Thus, $\delta = \angle\mathrm{FGH}$ when S and T in Fig. 2(c) become one point. Then

$$\tan\frac{\delta}{2} = \frac{1/2\overline{\mathrm{FH}}}{1/2\overline{\mathrm{EG}}} = \frac{\overline{\mathrm{FH}}}{\overline{\mathrm{EG}}}$$

Expressing $\overline{\mathrm{FH}}$ and $\overline{\mathrm{EG}}$ in terms of angles gives

$$\delta = 2\arctan\left(\frac{\sqrt{\dfrac{(-\cos\varphi_{\mathrm{f}})(1+\cos\theta_{\mathrm{f}})}{-2(\cos\varphi_{\mathrm{f}}+\cos\theta_{\mathrm{f}})}} + \sqrt{\dfrac{(1+\cos\varphi_{\mathrm{d}})(1+\cos\theta_{\mathrm{d}})}{-2(\cos\varphi_{\mathrm{d}}+\cos\theta_{\mathrm{d}})}}}{\sqrt{\dfrac{(1+\cos\varphi_{\mathrm{f}})(1+\cos\theta_{\mathrm{f}})}{-2(\cos\varphi_{\mathrm{f}}+\cos\theta_{\mathrm{f}})}} + \sqrt{\dfrac{(1+\cos\varphi_{\mathrm{d}})(1-\cos\theta_{\mathrm{d}})}{-2(\cos\varphi_{\mathrm{d}}+\cos\theta_{\mathrm{d}})}}} \cdot \sqrt{\frac{1-\cos\theta_{\mathrm{d}}}{1-\cos\varphi_{\mathrm{d}}}}\right) \tag{32}$$

This relationship is plotted in Fig. 5 when $\alpha = 7\pi/12$. Similar to the relationship between θ_{d} and θ_{f}, there are two values of δ for each θ_{f}.

It is interesting to note that among the rhombuses with the same side length, the square has the largest area, that is

$$\delta = \frac{\pi}{2} \tag{33}$$

Considering equation (32), equation (33) becomes

$$\left(\sqrt{\frac{(1+\cos\varphi_{\mathrm{f}})(1-\cos\theta_{\mathrm{f}})}{-2(\cos\varphi_{\mathrm{f}}+\cos\theta_{\mathrm{f}})}} + \sqrt{\frac{(1+\cos\varphi_{\mathrm{d}})(1-\cos\theta_{\mathrm{d}})}{-2(\cos\varphi_{\mathrm{d}}+\cos\theta_{\mathrm{d}})}}\right)^2 \frac{-(\cos\varphi_{\mathrm{d}}+\cos\theta_{\mathrm{d}})}{(1-\cos\theta_{\mathrm{d}})}$$
$$= \left(\sqrt{\frac{(1-\cos\varphi_{\mathrm{f}})(1+\cos\theta_{\mathrm{f}})}{-2(\cos\varphi_{\mathrm{f}}+\cos\theta_{\mathrm{f}})}} + \sqrt{\frac{(1-\cos\varphi_{\mathrm{d}})(1+\cos\theta_{\mathrm{d}})}{-2(\cos\varphi_{\mathrm{d}}+\cos\theta_{\mathrm{d}})}}\right)^2 \frac{-(\cos\varphi_{\mathrm{d}}+\cos\theta_{\mathrm{d}})}{(1-\cos\varphi_{\mathrm{d}})} \tag{34}$$

Considering equation (28), equation (34) can be simplified as

$$\tan^2\frac{\theta_{\mathrm{f}}}{2}\sec^2\frac{\theta_{\mathrm{d}}}{2} = \tan^2\frac{\theta_{\mathrm{d}}}{2} + \sec^2\alpha \tag{35}$$

When α, θ_{d}, and θ_{f} satisfy both equations (29) and (35), the fully deployed configuration of alternative form of the Bennett linkage is a square.

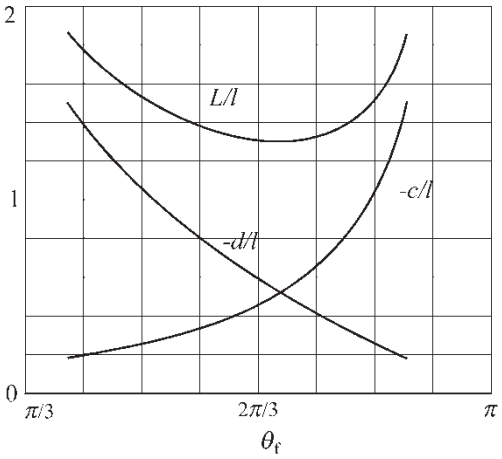

Fig. 4 θ_{f} versus L/l, $-c/l$, and $-d/l$ for $\alpha = 7\pi/12$

Solving equations (29) and (35)

$$\theta_{\mathrm{d}} = 2\theta_{\mathrm{f}} \tag{36}$$

and

$$\tan^2\alpha = \sec^2\theta_{\mathrm{f}}\left(\tan^2\frac{\theta_{\mathrm{f}}}{2} - 1\right) \tag{37}$$

are obtained.

The relationship of equation (37) is shown in Fig. 6, which is, in fact, the projection of the intersected curve between the surfaces of equations (29) and (35). Also, very interestingly, for any square fully deployed configuration

$$L = \sqrt{2}l \tag{38}$$

based on equations (29), (31), and (35).

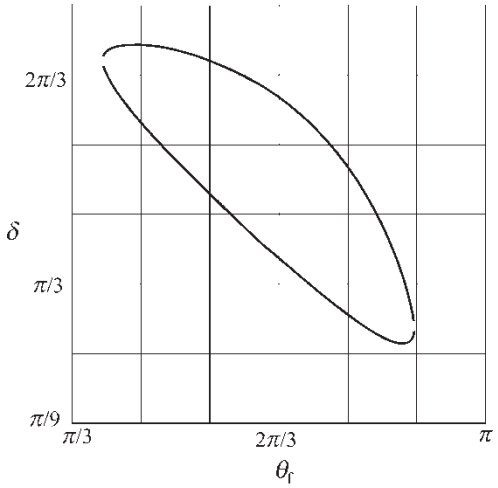

Fig. 5 θ_f versus δ for $\alpha = 7\pi/12$

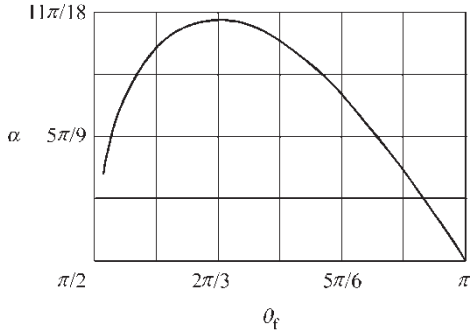

Fig. 6 α versus θ_f when the fully deployed structure based on the alternative form of the Bennett linkage forms a square

A few models of the Bennett linkage in its alternative forms have been built to verify the derivations presented here, one of which is shown in Fig. 7.

Finally, for a given α, there are two sets of θ_d and θ_f, in which configuration of the corresponding alternative form of Bennett linkage is square. However, when

$$\alpha = \arccos\frac{1}{3} \quad \text{or} \quad \pi - \arccos\frac{1}{3}$$

there is only one solution

$$\theta_f = \frac{2}{3}\pi \quad \text{and} \quad \theta_d = \frac{4}{3}\pi$$

In this case

$$c = d = \frac{\sqrt{6}}{4}l, \quad L = \sqrt{2}l$$

4 CONCLUSION

In this paper, a concept of utilizing the Bennett linkage for the construction of deployable structures has been presented. It has been found that the linkage in the alternative forms can achieve compact folding while maintaining the maximum expansion, and therefore, it becomes a good building block for the deployable structure. Detailed mathematical derivation has been given leading to the alternative formation.

In the derivation, only equilateral Bennett linkage satisfying equations (5) and (6) is considered. This is because Bennett [**16**] proved that all four hinge axes of the Bennett linkage can be regarded as generators of the same regulus on a certain hyperboloid at any configuration of the linkage. Hence, extensions of the opposite pair of the revolute axes of the non-equilateral Bennett linkage do not meet each other in a general configuration. Thus, the linkages in any alternative form cannot provide any advantage in terms of folding.

The authors have built models on the basis of the alternative forms of the Bennett linkage, all of which, including that shown in Fig. 7, have demonstrated that the derivation is correct. The way that this and other models are constructed and possibility of forming a large grid of Bennett linkages in their alternative forms are discussed in detail in part 2 of the article.

It should be pointed out that one of the alternative forms of the Bennett linkage capable of being folded compactly existed before this study. Pellegrino *et al.* [**18**] of Cambridge University first proposed such a

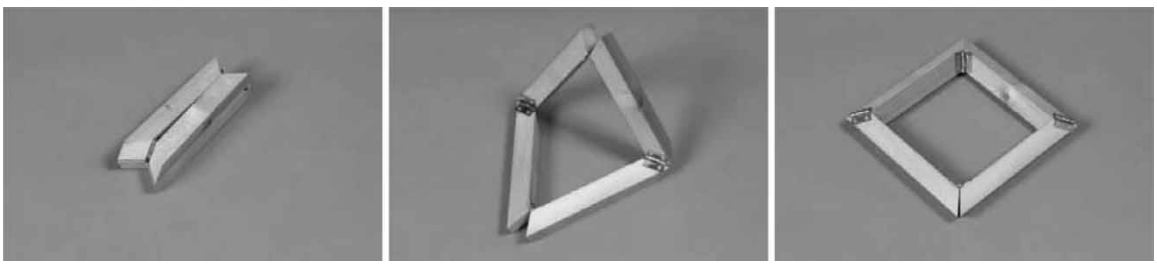

Fig. 7 Deployment sequence of a model. A Bennett linkage in its alternative form folded up in a compact bundle initially being expanded into a square frame

model. However, our study has found the complete set of solutions with identical features, providing much greater choice to designers of deployable structures.

ACKNOWLEDGEMENTS

The authors would like to express their gratitude to Prof. S. Pellegrino of the University of Cambridge for exposing this exciting mechanism. This work is supported by the Engineering and Physics Research Council in the form of a research grant (GR/M61207). Y. Chen would like to thank the University of Oxford for a graduate student scholarship.

REFERENCES

1 **Fang, H., Lou, M., Huang, J., Quijano, U.,** and **Pelaez, G.** Development of a 7-meter inflatable reflectarray antenna. AIAA paper 2004-1502, the 45th AIAA/ASME/ASCE/AHS/ASC Structures, Structural Dynamics and Materials Conference, Palm Springs, CA, USA, 2004.

2 **Miura, K.** *Variable geometry truss concept.* Institute of Space and Astronautical Science Report, No. 614, Japan, 1984.

3 **Fanning, P.** and **Hollaway, L. C.** The deployment analysis of a large space antenna. *Int. J. Space Struct.*, 1983, **8**(3), 209–220.

4 **Rogers, C. A., Stutzman, W. L., Campbell, T. G.,** and **Hedgepeth, J. M.** Technology assessment and development of large deployable antennas. *J. Aerospace Eng.*, 1993, **6**(1), 34–54.

5 **You, Z.** and **Pellegrino, S.** Cable-stiffened pantographic deployable structures. Part 2: mesh reflector. *AIAA J.*, 1997, **35**, 1348–1355.

6 **Adams, L. R.** The x-beam as a deployable boom for the space station. Proceedings of the 22nd Aerospace Mechanisms Symposium, NASA Langley Research Center, Hampton, Virginia, 1988, pp. 59–66.

7 **Bennett, G. T.** A new mechanism. *Engineering*, 1903, **76**, 777–778.

8 **Goldberg, M.** New five-bar and six-bar linkages in three dimensions. *Trans ASME*, 1943, **65**, 649–663.

9 **Waldron, K. J.** Hybrid overconstrained linkages. *J. Mech.*, 1968, **3**, 73–78.

10 **Wohlhart, K.** Merging two general Goldberg 5R linkages to obtain a new 6R space mechanism. *Mech. Mach. Theory*, 1991, **26**(2), 659–668.

11 **Mavroidis, C.** and **Roth, B.** Analysis and synthesis of overconstrained mechanism. Proceeding of the 1994 ASME Design Technical Conference, Minneapolis, MI, September, 1994, pp. 115–133.

12 **Diermeier, P.** A new 6R space mechanism. Proceeding 9th World Congress IFToMM, Milano, 1995, vol. 1, pp. 52–56.

13 **Chen, Y.** and **You, Z.** Network of Bennett linkages as deployable structures, AIAA 2001-4661. AIAA Space 2001 Conference and Exposition, Albuquerque, USA, 28–30 August 2001.

14 **Chen, Y.** and **You, Z.** Mobile assemblies based on the Bennett linkage. *Proc. Roy. Soc. A*, 2005, **461**, 1229–1245.

15 **Baker, J. E.** The Bennett, Goldberg and Myard linkages – in perspective. *Mech. Mach. Theory*, 1979, **14**, 239–253.

16 **Bennett, G. T.** The skew isogram mechanism. Proceedings of the London Mathematics Society, London, 2nd Series, 1914, vol. 13, pp. 151–173.

17 **Phillips, J.** *Freedom of machinery*, vol. II, 1990 (Cambridge University Press, Cambridge).

18 **Pellegrino, S., Green, C., Guest, S. D.,** and **Watt, A.** *SAR advanced deployable structure.* Technical Report, Department of Engineering, University of Cambridge, 2000.